

This dataset contains:

Analytical characterisation of the new ligands and the complexes (CHN microanalysis)

^1H and ^{13}C NMR spectra of the new organic ligands (raw data and plotted spectra).

Paramagnetic ^1H NMR spectra of the iron complexes (raw data and plotted spectra).

Electrospray mass spectra (plotted spectra).

X-ray Crystallographic data:

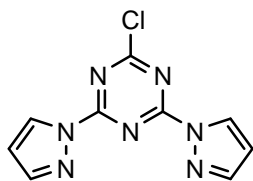
- Structure of L^1 (CCDC 1504278).
- Structure of L^3 (CCDC 1504279).
- Structure of $\text{L}^4 \cdot \text{CH}_2\text{Cl}_2$ (CCDC 1504280).
- Structure of L^5 (CCDC 1546568).
- Structure of L^6 (CCDC 1504281).
- Structure of L^8 (CCDC 1504282).
- Structure of $\alpha\text{-}[\text{Fe}(\text{L}^2)][\text{BF}_4]_2$ (CCDC 1504283).
- Structure of $\beta\text{-}[\text{Fe}(\text{L}^2)][\text{BF}_4]_2$ (CCDC 1504284).
- Unit cell determination of $[\text{Fe}(\text{L}^2)][\text{ClO}_4]_2$.
- Structure of $[\text{Fe}(\text{L}^3)_2][\text{BF}_4]_2 \cdot 2\text{CH}_2\text{Cl}_2$ (CCDC 1504285).
- Structure of $[\text{Fe}(\text{L}^4)_2][\text{BF}_4]_2 \cdot 1.55\text{CH}_3\text{CN} \cdot 0.45\text{CH}_2\text{Cl}_2$ (CCDC 1504286).
- Structure of $[\text{Fe}(\text{L}^5)_2][\text{BF}_4]_2 \cdot \frac{1}{2}\text{CH}_3\text{CN}$ (CCDC 1504287).
- Structure of $[\text{Fe}(\text{L}^6)_2][\text{BF}_4]_2 \cdot \frac{1}{2}\text{CH}_2\text{Cl}_2$ (CCDC 1504288).
- Structure of $[\text{Fe}(\text{L}^6)_2][\text{BF}_4]_2 \cdot n\text{CH}_2\text{Cl}_2$ ($n \approx 0.57$; CCDC 1534692).
- Structure of $[\text{Fe}(\text{L}^7)_2][\text{BF}_4]_2$ (CCDC 1502196).
- Structure of $[\text{Fe}(\text{L}^8)_2][\text{BF}_4]_2$ (CCDC 1504289).

X-ray powder diffraction data (measured and simulated).

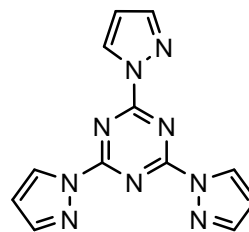
Solid state magnetic susceptibility measurements (raw and processed data).

Solution magnetic susceptibility data.

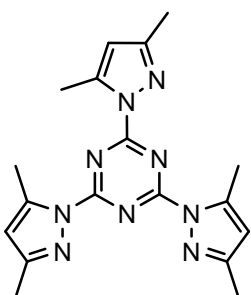
Ligands prepared during this study



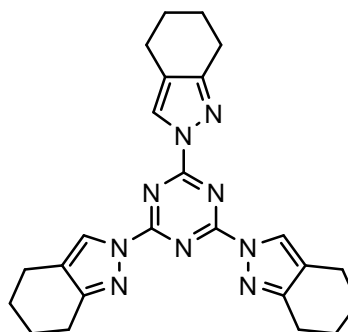
2,4-Di(pyrazol-1-yl)-6-chloro-1,3,5-triazine
 $C_9H_6ClN_7$
 L^1



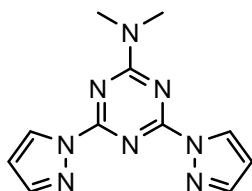
2,4,6-Tri(pyrazol-1-yl)-1,3,5-triazine
 $C_{12}H_9N_9$
 L^2



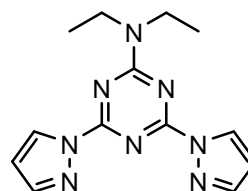
2,4,6-Tri(3,5-dimethylpyrazol-1-yl)-1,3,5-triazine
 $C_{18}H_{21}N_9$
 L^3



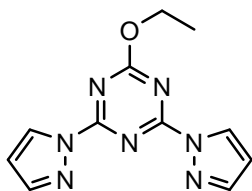
2,4,6-Tri(4,5,6,7-tetrahydroindazol-2-yl)-1,3,5-triazine
 $C_{24}H_{27}N_9$
 L^4



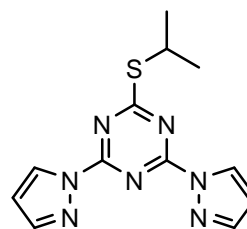
2,4-Di(pyrazol-1-yl)-6-(dimethylamino)-1,3,5-triazine
 $C_{11}H_{12}N_8$
 L^5



2,4-Di(pyrazol-1-yl)-6-(diethylamino)-1,3,5-triazine
 $C_{13}H_{16}N_8$
 L^6

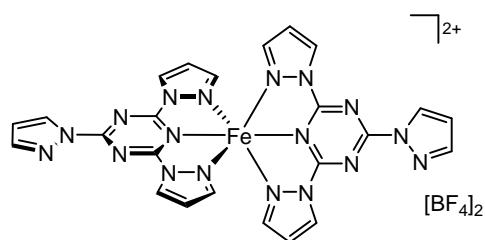


2,4-Di(pyrazol-1-yl)-6-ethoxy-1,3,5-triazine
 $C_{11}H_{11}N_7O$
 L^7

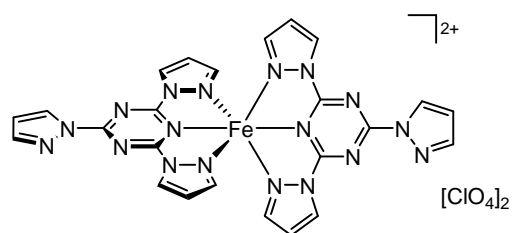


2,4-Di(pyrazol-1-yl)-6-(isopropylsulfanyl)-1,3,5-triazine
 $C_{12}H_{13}N_7S$
 L^8

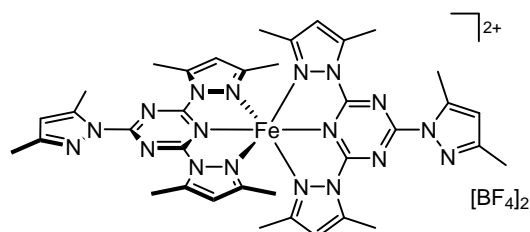
Complexes prepared during this study



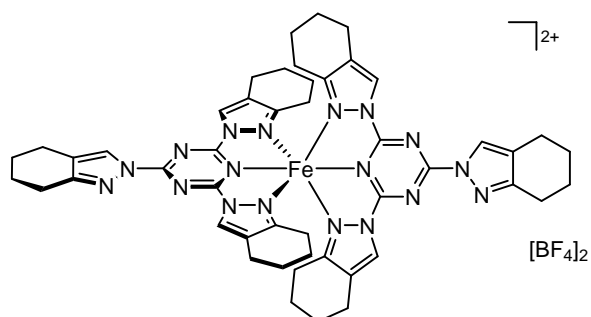
Bis-[2,4,6-tri(pyrazol-1-yl)-1,3,5-triazine]iron(II)
di-tetrafluoroborate
C₂₄H₁₈B₂F₈FeN₁₈
[Fe(L²)₂][BF₄]₂



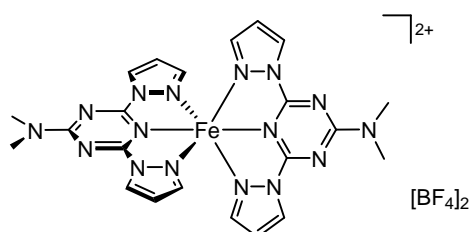
Bis-[2,4,6-tri(pyrazol-1-yl)-1,3,5-triazine]iron(II) diperchlorate
C₂₄H₁₈Cl₂FeN₁₈O₈
[Fe(L²)₂][ClO₄]₂



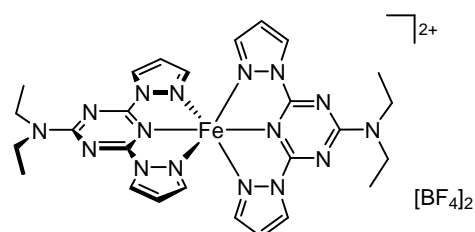
Bis-[2,4,6-tri(3,5-dimethylpyrazol-1-yl)-1,3,5-triazine]iron(II)
di-tetrafluoroborate
C₃₆H₄₂B₂F₈FeN₁₈
[Fe(L³)₂][BF₄]₂



Bis-[2,4,6-tri(4,5,6,7-tetrahydroindazol-2-yl)-1,3,5-triazine]iron(II)
di-tetrafluoroborate
C₄₈H₅₄B₂F₈FeN₁₈
[Fe(L⁴)₂][BF₄]₂

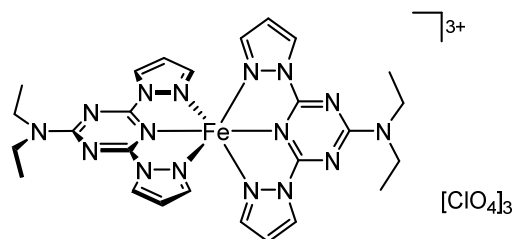


Bis-[2,4-di(pyrazol-1-yl)-6-(dimethylamino)-1,3,5-triazine]iron(II)
di-tetrafluoroborate
C₂₂H₂₄B₂F₈FeN₁₆
[Fe(L⁵)₂][BF₄]₂

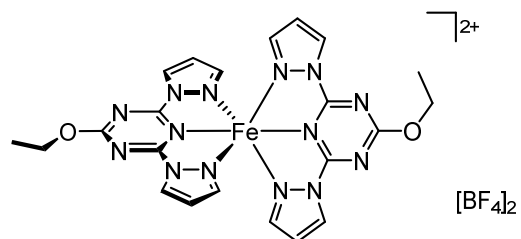


Bis-[2,4-di(pyrazol-1-yl)-6-(diethylamino)-1,3,5-triazine]iron(II)
di-tetrafluoroborate
C₂₆H₃₂B₂F₈FeN₁₆
[Fe(L⁶)₂][BF₄]₂

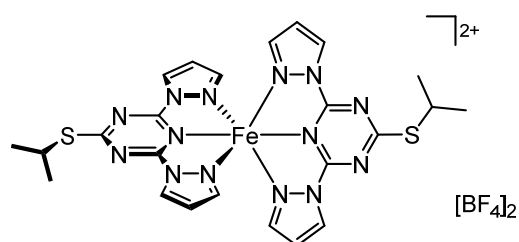
Complexes prepared during this study (continued)



Bis-[2,4-di(pyrazol-1-yl)-6-(diethylamino)-1,3,5-triazine]iron(III)
triperchlorate
C₂₆H₃₂Cl₃FeN₁₆O₁₂
[Fe(L⁶)₂][ClO₄]₃

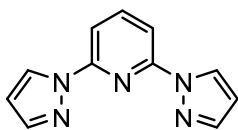


Bis-[2,4-di(pyrazol-1-yl)-6-ethoxy-1,3,5-triazine]iron(II)
di-tetrafluoroborate
C₂₂H₂₂B₂F₈FeN₁₄O₂
[Fe(L⁷)₂][BF₄]₂

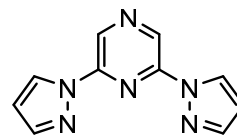


Bis-[2,4-di(pyrazol-1-yl)-6-(isopropylsulfanyl)-1,3,5-triazine]iron(II)
di-tetrafluoroborate
C₂₄H₂₆B₂F₈FeN₁₄S₂
[Fe(L⁸)₂][BF₄]₂

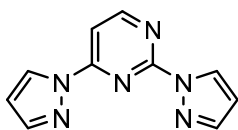
Ligands and complexes studied computationally



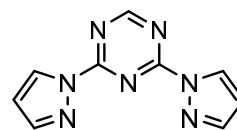
2,6-Di(pyrazol-1-yl)pyridine
 $C_{11}H_9N_5$
 bpp



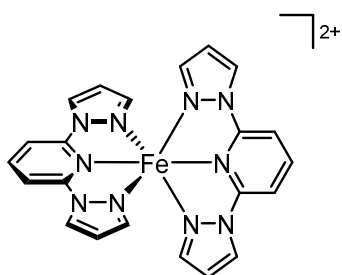
2,6-Di(pyrazol-1-yl)pyrazine
 $C_{10}H_8N_6$
 bpyz



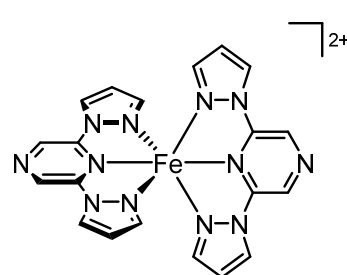
2,6-Di(pyrazol-1-yl)pyrimidine
 $C_{10}H_8N_6$
 bpym



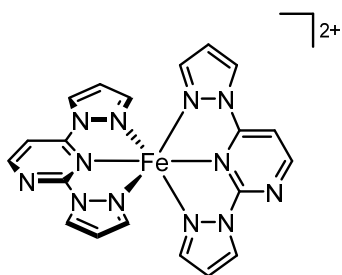
2,4-Di(pyrazol-1-yl)-1,3,5-triazine
 $C_9H_7N_7$
 bpt



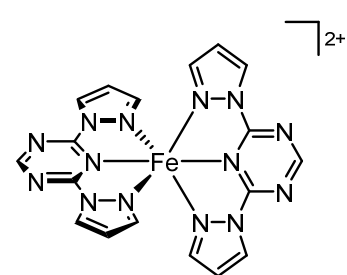
Bis-[2,6-di(pyrazol-1-yl)-pyridine]iron(II)
 $[C_{22}H_{18}FeN_{10}]^{2+}$
 $[Fe(bpp)_2]^{2+}$



Bis-[2,6-di(pyrazol-1-yl)-pyrazine]iron(II)
 $[C_{20}H_{16}FeN_{12}]^{2+}$
 $[Fe(bpyz)_2]^{2+}$

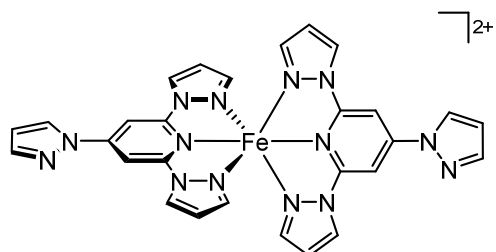


Bis-[2,6-di(pyrazol-1-yl)-pyrimidine]iron(II)
 $[C_{20}H_{16}FeN_{12}]^{2+}$
 $[Fe(bpym)_2]^{2+}$

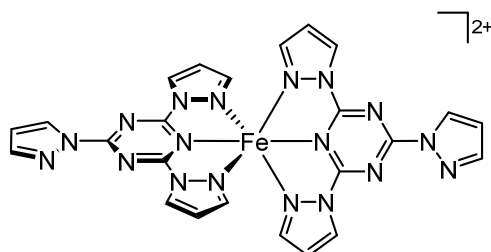


Bis-[2,4-di(pyrazol-1-yl)-1,3,5-triazine]iron(II)
 $[C_{18}H_{14}FeN_{14}]^{2+}$
 $[Fe(bpt)_2]^{2+}$

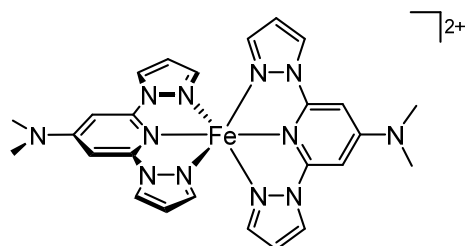
Ligands and complexes studied computationally (continued)



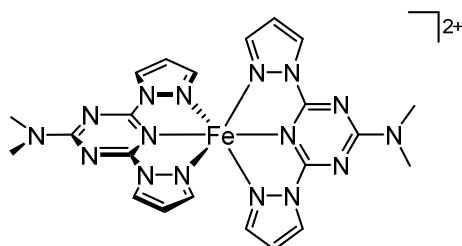
Bis-[2,4,6-tri(pyrazol-1-yl)-pyridine]iron(II)
 $[C_{28}H_{22}FeN_{14}]^{2+}$
 $[Fe(tpp)_2]^{2+}$



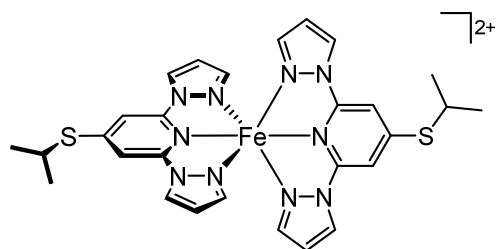
Bis-[2,4,6-tri(pyrazol-1-yl)-1,3,5-triazine]iron(II)
 $[C_{24}H_{18}B_2F_8FeN_{18}]^{2+}$
 $[Fe(L^2)_2]^{2+}$



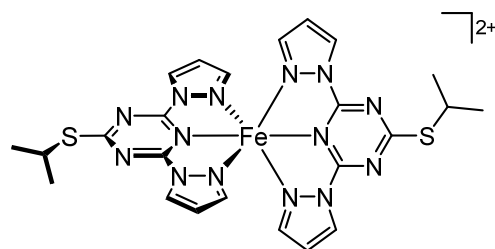
Bis-[2,6-di(pyrazol-1-yl)-4-dimethylaminopyridine]-
 iron(II)
 $[C_{28}H_{22}FeN_{14}]^{2+}$
 $[Fe(bpp^{NMe_2})_2]^{2+}$



Bis-[2,4-di(pyrazol-1-yl)-6-(dimethylamino)-1,3,5-triazine]-
 iron(II)
 $[C_{22}H_{24}B_2F_8FeN_{16}]^{2+}$
 $[Fe(L^5)_2]^{2+}$



Bis-[2,6-di(pyrazol-1-yl)-4-(isopropylsulfanyl)pyridine]-
 iron(II)
 $[C_{28}H_{30}FeN_{10}S_2]^{2+}$
 $[Fe(bpp^{SiPr})_2]^{2+}$



Bis-[2,4-di(pyrazol-1-yl)-6-(isopropylsulfanyl)-1,3,5-triazine]-
 iron(II)
 $[C_{24}H_{26}FeN_{14}S_2]^{2+}$
 $[Fe(L^8)_2]^{2+}$